Randomly Distributed Delayed Communication and Coherent Swarm Patterns

Brandon Lindley,
NRC postodctoral fellow at the US Naval Research Labooratory, Code 6792, Washington, DC 20375 USA

Luis Mier-y-Teran-Romero, and
NIH post doctoral fellow at the Naval Research Laboratory

Ira B. Schwartz
US Naval Research Labooratory, Code 6792, Washington, DC 20375 USA

Brandon Lindley: brandon.lindley.ctr@nrl.navy.mil; Luis Mier-y-Teran-Romero: luis.miery@nrl.navy.mil; Ira B. Schwartz: Ira.schwartz@nrl.navy.mil

Abstract

Previously we showed how delay communication between globally coupled self-propelled agents causes new spatio-temporal patterns to arise when the delay coupling is fixed among all agents [1]. In this paper, we show how discrete, randomly distributed delays affect the dynamical patterns. In particular, we investigate how the standard deviation of the time delay distribution affects the stability of the different patterns as well as the switching probability between coherent states.

I. INTRODUCTION

Numerous recent investigations have been devoted to the study of interacting multi-agent or swarming systems in various natural and engineering fields of study. Investigations of interacting systems have revealed the emergence of highly complex dynamic behaviors in space and time which arise even though the dynamics of a single agent is quite simple [2]. In particular, these multi-agent swarms can self-organize in complicated spatio-temporal patterns that depend on the details of the inter-agent interactions. These investigations have been motivated by and had an impact on many diverse biological systems such as bacterial colonies, schooling fish, flocking birds, swarming locusts, ants, and pedestrians [3], [4], [5], [6], [7]. In this paper, we are interested in the application that biological analogies have on the design of systems of autonomous, inter-communicating robotic systems [8], [9], [10], [11] and mobile sensor networks [12].

There is great interest to design agent-interaction protocols to carry out robotic motion planning, consensus and cooperative control, and spatio-temporal formation. One methodology is to combine inter-agent potentials with external ones in order to achieve multi-agent cooperative motion in a manner that is not too sensitive with respect the number of agents. Some important applications making use of scalable numbers of agents are: obstacle avoidance [10], boundary tracking [13], [14], environmental sensing [12], [15], decentralized target tracking [16], environmental consensus estimation [12], [17] and task allocation [18].

Authors have employed very diverse approaches in the study of multi-agent systems. Some authors have described the swarms at the individual level, writing their models in terms of ordinary differential equations (ODEs) or delay differential equations (DDEs) to describe their trajectories [19], [20], [9]. The addition of noise on the swarm's dynamics introduces even richer behavior, such as noise-induced transitions between different coherent patterns [2], [1]. The study of noisy swarm dynamics has benefited from tools from statistical physics applied to both first and second order phase transitions that have been found in the formation of coherent states [21].

One important aspect of the understanding and design of space-time behavior in communicating robotic systems is that of time delay. Time delay arises in latent communication between agents, as well as actuation lag times due to inertia. Time delays can have interesting and surprising dynamical consequences in a system, such as large-scale synchronization [22], [23], [24], and have been used successfully for control purposes [25], [26]. Many of the initial time-delay studies focused on the case of one or a few discrete time delays. Recently, more complex situations have been considered such as the case of having several [27] and random time-delays [28], [29]. Another interesting case is that of distributed time delays, i.e. when the dynamics of the system depends on a continuous interval in its past instead of on a discrete instant [30].

In the case of swarming systems in stochastic environments, it has been observed that the introduction of a discrete communication time delay induces a transition from one spatio-temporal pattern to another as the time delay passes a certain threshold [1]. It was shown in [1] how the complex interplay exists between the attractive coupling and the time delay in the transitions between different spatio-temporal patterns [31], [32]. Time delays in robotic systems have been also studied in the contexts of consensus estimation [17] and task allocation [18]; in the latter, the time delays originate from the period of time required to switch between different tasks.

In this paper, we consider a swarming model with discrete, randomly distributed time delays. We explicitly show how a distribution of delay times perturb the dynamics from the single discrete case delay case analytically. We illustrate the dynamical effects of delay distributions with varying width and show that the system is bistable, and very sensitive to choice of initial starting conditions.

II. Swarm Model

We investigate the dynamics of a two-dimensional system of N identical self-propelling agents that are attracted to each other in a symmetric manner. We consider the attraction between agents to occur in a time-delayed fashion, due to the finite communication speeds and information-processing times. Specifically, we focus on the situation in which the time-delay is nonuniform across agents: there is one time delay for every pair of agents $\tau_{ij}(=\tau_{ji})$, for particles i and j. The time delays τ_{ij}'s are time-independent and are drawn independently from a random distribution $\rho_\tau(\tau)$. The swarm dynamics are described by the following governing equations:

$$\dot{\mathbf{r}}_i = \mathbf{v}_i, \quad \text{(1a)}$$

$$\dot{\mathbf{v}}_i = (1-|\mathbf{v}_i|^2)\mathbf{v}_i - \frac{a}{N}\sum_{\substack{j=1 \\ i \neq j}}^{N} (\mathbf{r}_i(t) - \mathbf{r}_j(t-\tau_{ij})), \quad \text{(1b)}$$

for $i = 1,2\ldots, N$. The position and velocity of the ith agent at time t are denoted by $\mathbf{r}_i$ and $\mathbf{v}_i$, respectively. Each agent has self-propulsion and frictional drag forces given by the expression term $(1 - |\mathbf{v}_i|^2)\,\mathbf{v}_i$. The coupling constant a measures the strength of the attraction between agents and the communication time delay between particles i and j is given by τ_{ij}. Note that in the absence of coupling agents tend to move in a straight line with unit speed as time tends to infinity.

III. Mean Field Approximation

We carry out a mean field approximation of the swarming system by switching to particle coordinates relative to the center of mass and disregarding the noise terms. The center of mass of the swarming system is given by

$$\mathbf{R}(t)=\frac{1}{N}\sum_{i=1}^{N}\mathbf{r}_i(t). \quad (2)$$

We can decompose the position of each particle into

$$\mathbf{r}_i=\mathbf{R}+\delta\mathbf{r}_i, \quad i=1,2\ldots,N, \quad (3)$$

where we'll have

$$\sum_{i=1}^{N}\delta\mathbf{r}_i(t)=0. \quad (4)$$

Inserting Eq. (3) into the second order system equivalent to Eq. (1) and simplifying we get

$$\ddot{\mathbf{R}}+\delta\ddot{\mathbf{r}}_i=(1-|\dot{\mathbf{R}}|^2-2\,\dot{\mathbf{R}}\cdot\delta\dot{\mathbf{r}}_i-|\delta\dot{\mathbf{r}}_i|^2)\,(\dot{\mathbf{R}}+\delta\dot{\mathbf{r}}_i)-\frac{a(N-1)}{N}\,(\mathbf{R}(t)+\delta\mathbf{r}_i(t))+\frac{a}{N}\sum_{\substack{j=1\\ i\neq j}}^{N}(\mathbf{R}(t-\tau_{ij})+\delta\mathbf{r}_j(t-\tau_{ij})), \quad (5)$$

Summing Eq. (5) over i and using Eq. (4), we get

$$\ddot{\mathbf{R}}=\left(1-|\dot{\mathbf{R}}|^2-\frac{1}{N}\sum_{i=1}^{N}|\delta\dot{\mathbf{r}}_i|^2\right)\dot{\mathbf{R}}-\frac{1}{N}\sum_{i=1}^{N}(2\,\dot{\mathbf{R}}\cdot\delta\dot{\mathbf{r}}_i+|\delta\dot{\mathbf{r}}_i|^2)\,\delta\dot{\mathbf{r}}_i-a\frac{N-1}{N}\mathbf{R}(t)+\frac{a}{N^2}\sum_{i=1}^{N}\sum_{\substack{j=1\\ i\neq j}}^{N}(\mathbf{R}(t-\tau_{ij})+\delta\mathbf{r}_j(t-\tau_{ij})). \quad (6)$$

We now make some approximations on the terms with the double sums. For the displacements from the center of mass, we have

$$\begin{aligned}\tfrac{a}{N^2}\sum_{i=1}^{N}\sum_{\substack{j=1\\ i\neq j}}^{N}\delta\mathbf{r}_j(t-\tau_{ij}) &= \tfrac{a(N-1)}{N^2}\sum_{j=1}^{N}\tfrac{1}{N-1}\sum_{\substack{j=1\\ i\neq j}}^{N}\delta\mathbf{r}_j(t-\tau_{ij}) \\ &\approx \tfrac{a(N-1)}{N^2}\int_0^\infty\sum_{j=1}^{N}\delta\mathbf{r}_j(t-\tau)\rho_\tau(\tau)d\tau=0,\end{aligned} \quad (7)$$

since $\sum_{j=1}^{N}\delta\mathbf{r}_j(t-\tau)=0$ by Eq. (4). In passing from the discrete to the continuous averaging above, we argue as follows. The expression $\frac{1}{N-1}\sum_{i=1 i\neq j}^{N}\delta\mathbf{r}_j(t-\tau_{ij})$ is the average of $\delta\mathbf{r}_j(t)$ at the $N-1$ times $t-\tau_{ij}$. Since $N\gg 1$ and the times τ_{ij} are distributed with density $\rho_\tau(\tau)$, this is approximately equal to $\int_0^\infty \delta\mathbf{r}_j(t-\tau)\rho_\tau(\tau)d\tau$.

Similarly,

$$\frac{a}{N^2}\sum_{i=1}^{N}\sum_{\substack{j=1\\ i\neq j}}^{N}\mathbf{R}(t-\tau_{ij})\approx\frac{a(N-1)}{N}\int_0^\infty\mathbf{R}(t-\tau)\rho_\tau(\tau)d\tau. \quad (8)$$

In a purely heuristic manner, we neglect all fluctuation terms $\delta\mathbf{r}_j(t)$ in the dynamics of the center of mass and obtain the mean field approximation:

$$\ddot{\mathbf{R}}=(1-|\dot{\mathbf{R}}|^2)\,\dot{\mathbf{R}}-a\,(\mathbf{R}(t)-\int_0^\infty\mathbf{R}(t-\tau)\rho_\tau(\tau)d\tau)\,. \quad (9)$$

where we approximated $\frac{N-1}{N}\approx 1$, since we are considering large numbers of agents.

IV. Bifurcations in the Mean Field Equation

The behavior of the system in the mean field approximation in different regions of parameter space may be better understood by using bifurcation analysis. This mathematical technique will allow us to show how the parameter plane of coupling constant a and mean time delay μ_τ is divided into regions with different dynamical behaviors.

First we show that Eq. (9) has a uniformly translating solution $\mathbf{R}(t) = \mathbf{R}_0 + \mathbf{V}_0 \cdot t$, where $\mathbf{R}_0$ and $\mathbf{V}_0$ are constant, two-dimensional vectors. Inserting the uniformly translating state into Eq. (9), we get

$$0=(1-|\mathbf{V}_0|^2)\,\mathbf{V}_0-a\int_0^\infty\tau\rho_\tau(\tau)d\tau\,\mathbf{V}_0, \quad (10)$$

since $\int_0^\infty\rho_\tau(\tau)d\tau=1$. Hence, the speed $|\mathbf{V}_0|$ of the uniformly translating state must satisfy

$$|\mathbf{V}_0|^2=1-a\int_0^\infty\tau\rho_\tau(\tau)d\tau=1-a\mu_\tau, \quad (11)$$

where μ_τ is the mean of the ρ_τ distribution. We note that the direction of motion and starting point $\mathbf{R}_0$ are arbitrary.

The other state of interest is the stationary state $\mathbf{R}(t) = \mathbf{R}_0$, for an arbitrary constant vector $\mathbf{R}_0$. In the two-parameter space (a, μ_τ), the hyperbola $a\mu_\tau = 1$ is in fact a pitchfork bifurcation line on which the uniformly translating states are born from the stationary state.

The linear stability of the stationary state is determined by the solutions to the characteristic equation of Eq. (9):

$$\mathscr{D}(\lambda)=a\left(1-\int_0^\infty\rho_\tau(\tau)e^{-\lambda\tau}d\tau\right)-\lambda+\lambda^2=0, \quad (12)$$

and so involves the Laplace transform of the distribution ρ_τ.

In our numerical simulations of system (1), we considered a truncated Gaussian distribution:

$$\rho_\tau = \begin{cases} \mathcal{N} e^{\frac{(\tau-\tau_0)^2}{2\tau_1^2}} & \text{if } \tau \geq 0 \\ 0 & \text{if } \tau < 0, \end{cases} \quad (13)$$

where $\mathcal{N}$ is the normalization constant. Note that because of the truncation, τ_0 and τ_1 are only approximately equal to the mean and standard deviation of ρ_τ and $\mathcal{N}$ is only approximately $1/\sqrt{2\pi\tau_1^2}$.

We approximate the Laplace transform of the truncated Gaussian distribution by extending the integration range to the whole real line and taking $\mathcal{N} \approx \sqrt{2\pi\tau_1^2}$. In addition, we approximate the mean and standard deviation of ρ_τ as $\mu_\tau \approx \tau_0$ and $\sigma_\tau \approx \tau_1$, respectively. The result is

$$\int_0^\infty \rho_\tau(\tau) e^{-\lambda\tau} d\tau \approx e^{\lambda\mu_\tau + \lambda^2\sigma_\tau^2/2}. \quad (14)$$

We use the above approximation to the Laplace transform of ρ_τ to search for Hopf bifurcation curves in the (a, μ_τ) plane, by taking $\lambda = i\omega$ in the characteristic equation (12). The equation $\mathcal{D}(i\omega) = 0$ is equivalent to:

$$a - \omega^2 - i\omega = a e^{i\omega\mu_\tau - \omega^2\sigma_\tau^2/2}, \quad (15)$$

from which we obtain the Hopf curves parameterized by ω:

$$a_H(\omega) = \frac{\omega\left(\omega \pm \sqrt{e^{-\sigma_\tau^2\omega^2}(1+\omega^2) - 1}\right)}{1 - e^{-\sigma_\tau^2\omega^2}}, \quad (16a)$$

$$\mu_{\tau H}(\omega) = \frac{1}{\omega}\left(\arctan\left(\frac{\omega}{a_H(\omega) - \omega^2}\right) + 2n\pi\right), n = 0, 1, \ldots. \quad (16b)$$

In the above expression for $\mu_{\tau H}(\omega)$, the branch of tan in $(0, \pi)$ should be used, since the complex number on the left hand side of Eq. (15) is always on the top half plane. This family of Hopf curves labeled by n, together with the pitchfork bifurcation curve $a\mu_\tau = 1$ are shown in Figure 1, for various values of σ_τ.

When $\sigma_\tau = 0$, the system exhibits a degenerate point at $a = 1/2$, $\mu_\tau = 2$ (Fig. 1(a)), where the Hopf bifurcation frequency becomes zero. This is similar, but not equivalent to a Bogdanov-Takens bifurcation as is known from previous work [31], [32]. Since the point on the Hopf curve in a two-parameter bifurcation plane occurs when the Hopf frequency becomes zero, we define this point as a Zero Frequency Hopf (ZFH) point.

For $\sigma_\tau > 0$, this ZFH point shifts and a second ZFH point appears at $a \to \infty$ and $\mu_\tau \to 0$. The location of the two ZFH points in the (a, μ_τ), plane is given by ($a_{ZFH}^{(\pm)}, 1/a_{ZFH}^{(\pm)}$), where $a_{ZFH}^{(\pm)} = \frac{1}{\sigma_\tau^2}(1 \pm \sqrt{1-\sigma_\tau^2})$.

When $\sigma_\tau = 0$, the behavior of the mean field in the vicinity of the ZFH point is relatively well understood [32], [31] and is as follows (see Fig. 1(a)). In the region between the

pitchfork and the first member of the Hopf family, the stationary state is stable. A simulation of the full system (1) with parameters in this area reveals that indeed the center of mass of the agents comes to rest as time progresses and the particles spread themselves along a ring with radius $1/\sqrt{a}$. Roughly half of the particles move clockwise and the other half counterclockwise. Along the first Hopf curve, a stable limit cycle is born and the center of mass begins to oscillate periodically on a circular orbit. Below the pitchfork bifurcation curve $a\mu_\tau = 1$, the translating state is stable. Finally, we mention that there is a region of bistability in the parameter region above the ZFH point (1/2, 2) between the pitchfork curve $a\mu_\tau = 1$ and the curve $a\mu_\tau^2 = 2$ (not shown), where the center of mass can either translate or rotate. On the curve $a\mu_\tau^2 = 2$ there is a global bifurcation where the radius of the orbit diverges and the limit cycle disappears.

The above discussion helps us understand the bifurcation planes in Figs. 1(b) through 1(d). Most significantly, we see that the parameter region where the stationary state is stable decreases in size as the width of the time delay distribution widens. Hence the system has a higher tendency to behave in an oscillatory manner for wider time delay distributions. This effect has been corroborated in numerical simulations (results not shown).

V. Numerical Simulations

We analyze the dynamics of system (1) by solving the system of DDEs numerically. We use Heun's method together with quadratic Lagrange interpolation to evaluate the time-delayed terms of Eqs. (1). Overall, the numerical method is second order with respect to the step-size Δt. For all simulations we take the agents to be uniformly distributed in a random fashion within the unit box $0 \le x \le 1$ and $0 \le y \le 1$, and each particle is initially at rest $\mathbf{v}_j = 0$. Moreover, since we are interested in investigating the time-asymptotic behavior, for all numerical experiments the time of integration is long enough to allow transients to decay.

In [31], [32] it was shown that for the parameter set $a = 2$, $\tau = 2$ (fixed delay) that the system exhibited a bistable set of solutions. In the rotating state solution, all particles collapse to a point and that cluster of particles rotates around a fixed center in a circular orbit. The other possible stable solution is a ring state, in which all particles distribute themselves uniformly along a circle and orbit around its center at unit speed. Interestingly, not all particles traverse the ring in the same direction; roughly half move clockwise and half move anti-clockwise. We will now examine these two states, but with random delays given by the truncated Gaussian distribution in Eq. (13).

Figure 2 shows the two final particle distributions after transients in a simulation with an initial state of $N = 150$ randomly placed particles, and where $\mu_\tau = 2$ and $\sigma_\tau = 0.15$. In this case, depending upon the random selection of delays, either stable solution (ring or rotating) is possible. To understand the effects of increasing the standard deviation of the random delays, we use a Monte Carlo method. At 100 different values of σ_τ in the range $0 \le \sigma_\tau \le 0.5$, we generate random time delays from the distribution in Eq. (13), we then simulate the system starting from the same initial condition and we determine what state is acquired by the swarm in the long-time limit. To determine this, we first measure the time-averaged distance of particle j to the center of mass over the interval (t_1, t_2):

$$\langle \delta \mathbf{r}_j \rangle_{(t_1,t_2)} = \frac{1}{t_2 - t_1} \int_{t_1}^{t_2} |\delta \mathbf{r}_j(t)| dt \quad (17)$$

where the size of the interval (t_1, t_2) is long enough to include several periods of oscillation. The ensemble average of Eq. (17) is then

$$\langle \delta \mathbf{r} \rangle_{(t_1,t_2)} = \frac{1}{N} \sum_{j=1}^{N} \langle \delta \mathbf{r}_j \rangle_{(t_1,t_2)}. \quad (18)$$

A value $\langle \delta \mathbf{r} \rangle_{(t_1,t_2)} \sim 1/\sqrt{a}$ will indicate[1] that the system has converged to the ring state, while $\langle \delta \mathbf{r} \rangle_{(t_1,t_2)} \ll 1/\sqrt{a}$ shows that the rotating state has been adopted instead[2].

Figure 3(a) demonstrates the effect of increasing σ_τ on the final state. The blue circles show that for σ_τ small, this initial condition converges to the rotating state. However, for $\sigma_\tau \gtrsim 0.2$ the same initial collection of particles will converge to the ring state with high probability. In between, there is a transition region where both states are commonly observed; the state that occurs depends on the random choice of time delays. The black dashed lines of 3(a) show two simulations, one which starts near the rotating state (the lower curve), and one which starts near the ring state (the upper curve) as σ_τ is increased. These curves demonstrate the stability of these steady states, and the effect of random delays near these states.

Figure 3(b) shows the conditional probability of ending up in the ring state as a function of σ_τ. As expected, for this choice of initial conditions, for σ_τ small enough, there is zero probability of leaving the rotating state; however, as σ_τ is increased, the probability increases to one.

The results of these numerical studies strongly suggest that even though there is bi-stability between the ring and the rotating states, the size of their respective basins of attraction is changing dramatically as the standard deviation σ_τ increases.

VI. Discussion

In this paper we studied the dynamics of a self-propelling swarm with time-delayed inter-agent attraction. In contrast to the previously considered case of uniform time delay across agents, we considered the situation in which the time delay between every pair of agents is drawn randomly from a distribution ρ_τ.

Using a mean-field model of the swarm, we showed how the two parameter bifurcation plane of coupling strength and mean time delay changes with respect to the case in which all time delays are equal. The full implications of these bifurcation results are the subject of our ongoing work. In particular, it is unclear what the stable solutions are. Nevertheless, the dramatic changes seen in the two parameter bifurcation plane as the standard deviation σ_τ increases suggest that the basins of attraction of each attractor undergo big changes as well.

Our numerical experiments show that the swarm displays bi-stable behavior between the ring and rotating states, at the parameters considered. Interestingly, however, our work suggests that the basin of attraction of the ring state greatly expands as the distribution of time-delays ρ_τ widens. Thus, in a sense, widening the distribution of time-delays stabilizes the stationary state of the swarm center of mass.

Even though in our model the attractive force among agents is linear, we believe this work is useful since it represents a first approximation for other, more general forms of attractive interaction. Here, we have limited our focus to the case where the delays between agents are

[1] When the delays are uniform, the ring state has a radius of $1/\sqrt{a}$ [32].
[2] This is true for the range of values of σ_τ considered here.

symmetric and constant. However, one important generalization of this system involves incorporating time dependent delays, including those which vary as a function of the distance between the two agents. This particular refinement of our model is the subject of ongoing work and beyond the scope of the current paper.

Finally, although we did not consider repulsion between agents, preliminary research leads us to believe that the patterns observed in this investigation persist when the characteristic repulsion strength between robots is small compared to global attraction parameters. For these reasons, our results indicate how to exploit time-delayed actuation when designing swarm robotic systems with desired tasks and functionalities.

Acknowledgments

This work was supported by the Office of Naval Research and the National institutes of Health.

The authors gratefully acknowledge the Office of Naval Research for their support. LMR and IBS are supported by Award Number R01GM090204 from the National Institute Of General Medical Sciences. The content is solely the responsibility of the authors and does not necessarily represent the official views of the National Institute Of General Medical Sciences or the National Institutes of Health. E.F. is supported by the Naval Research Laboratory (Award No. N0017310-2-C007).

References

1. Forgoston E, Schwartz I. Delay-induced instabilities in self-propelling swarms. Phy Rev E. 2008; 77
2. Erdmann U, Ebeling W. Noise-induced transition from translational to rotational motion of swarms. Phys Rev E. 2005; 71
3. Budrene E, Berg H. Dynamics of formation of symmetrical patterns by chemotactic bacteria. Nature. 1995; 376(6535):49–53. [PubMed: 7596432]
4. Toner J, Tu Y. Long-range order in a two-dimensional dynamical xy model: How birds fly together. Phys Rev Lett. 1995; 75(23):4326–4329. [PubMed: 10059876]
5. Parrish JK. Complexity, pattern, and evolutionary trade-offs in animal aggregation. Science. Apr. 1999 284:99–101. [PubMed: 10102827]
6. Topaz C, Bertozzi A. Swarming patterns in a two-dimensional kinematic model for biological groups. SIAM Journal on Applied Mathematics. 2004; 65(1):152–174.
7. Hebling D, Molnar P. Social force model for pedestrian dynamics. Phys Rev E. 1995; 51:4282–4286.
8. Leonard N, Fiorelli E. Virtual leaders, artificial potentials and coordinated control of groups. Proc of the 40th IEEE Conference on Decision and Control. 2002; 3:2968–2973.
9. Justh E, Krishnaprasad P. Steering laws and continuum models for planar formations. Proc of the 42nd IEEE Conference on Decision and Control. 2004; 4:3609–3614.
10. Morgan D, Schwartz I. Dynamic coordinated control laws in multiple agent models. Phys Lett A. 2005; 340(1–4):121–131.
11. Chuang, Y-L.; Huang, YR.; D'Orsogna, MR.; Bertozzi, AL. Multi-vehicle flocking: Scalability of cooperative control algorithms using pairwise potentials. Proc. of the 2007 IEEE International Conference on Robotics and Automation; 2007. p. 2292-2299.
12. Lynch KM, Schwartz P, Yang IB, Freeman RA. Decentralized environmental modeling by mobile sensor networks. IEEE Trans Robotics. 2008; 24(3):710–724.
13. Hsieh, C.; Jin, Z.; Marthaler, D.; Nguyen, B.; Tung, D.; Bertozzi, A.; Murray, R. Experimental validation of an algorithm for cooperative boundary tracking. Proc. of the 2005 American Control Conference; 2005. p. 1078-1083.
14. Triandaf I, Schwartz IB. A collective motion algorithm for tracking time-dependent boundaries. Mathematics and Computers in Simulation. 2005; 70:187–202.
15. Lu B, Oyekan J, Gu D, Hu H, Nia HFG. Mobile sensor networks for modelling environmental pollutant distribution. Int J Sys Sci. 2011; 42(9, SI):1491–1505.

16. Chung, T.; Burdick, J.; Murray, R. A decentralized motion coordination strategy for dynamic target tracking. Proc. 2006 Conference on International Robotics and Automation; 2006. p. 2416-22.
17. Papachristodoulou, A.; Jadbabaie, A. Synchronization in oscillator networks with heterogeneous delays, switching topologies and nonlinear dynamics. Proc. of the 45th IEEE Conference on Decision and Control; 2007. p. 4307-4312.
18. Mather TW, Hsieh MA. Macroscopic modeling of stochastic deployment policies with time delays for robot ensembles. Int J Robot Res. Apr.2011 30:590–600.
19. Vicsek T, Czirók A, Ben-Jacob E, Cohen I, Shochet O. Novel type of phase transition in a system of self-driven particles. Phys Rev Lett. 1995; 75(6):1226–1229. [PubMed: 10060237]
20. Flierl G, Grünbaum D, Levins S, Olson D. From individuals to aggregations: the interplay between behavior and physics. J Theor Biol. 1999; 196(4):397–454. [PubMed: 10036198]
21. Aldana M, Dossetti V, Huepe C, Kenkre V, Larralde H. Phase transitions in systems of self-propelled agents and related network models. Phys Rev Lett. 2007; 98
22. Englert A, Heiligenthal S, Kinzel W, Kanter I. Synchronization of chaotic networks with time-delayed couplings: An analytic study. Phys Rev E. Apr 26.2011 83
23. Zuo Z, Yang C, Wang Y. A unified framework of exponential synchronization for complex networks with time-varying delays. Phys Lett A. Apr 19.2010 374:1989–1999.
24. Hache A. Synchronization with sound propagation delays. EPL. Apr.2010 90
25. Atay, FM. Networks with delays. In: Feng, J.; Jost, J.; Qian, MP., editors. Networks: From Biology to Theory; Sino, German International Conference on Networks - From Biology to Theory; Beijing, Peoples Rep. China. APR 04–08, 2005; 2007. p. 23-33.
26. Konishi K, Kokame H, Hara N. Stabilization of a steady state in network oscillators by using diffusive connections with two long time delays. Phys Rev E. Jan.2010 81
27. Ahlborn A, Parlitz U. Controlling spatiotemporal chaos using multiple delays. Phys Rev E. Jun. 2007 75
28. Wu D, Zhu S, Luo X. Cooperative effects of random time delays and small-world topologies on diversity-induced resonance. EPL. Jun.2009 86
29. Marti, AC.; Ponce, MC.; Masoller, C. Chaotic maps coupled with random delays: Connectivity, topology, and network propensity for synchronization. Physica A; 9th Latin American Workshop on Nonlinear Phenomena; San Carlos de Bariloche, Argentina. Oct 23–28, 2005; Nov 1. 2006 p. 104-107.
30. Omi T, Shinomoto S. Can distributed delays perfectly stabilize dynamical networks? Phys Rev E. Apr.2008 77
31. Mier-y Teran-Romero, L.; Forgoston, E.; Schwartz, IB. Noise, bifurcations, and modeling of interacting particle systems. IROS 2011 conference papers; accepted, 2011
32. Mier-y Teran-Romero, L.; Forgoston, E.; Schwartz, IB. IEEE TRO. Coherent pattern prediction in swarms of delay-coupled agents. submitted, 2011
33. Guckenheimer, J.; Holmes, P. Nonlinear Oscillations, Dynamical Systems, and Bifurcations of Vector Fields. 1. Berlin: Springer-Verlag; 1986.

VII. Appendix Video Description

The purpose of this research is to investigate the effects of randomized communication delay on emerging patterns in swarming dynamics. This short video captures the transition between two different stable patterns for a swarm as a function of the standard distribution of the delays.

The two coordinate axes in the video show a scatter plot of the positions of the particles animated in time. The initial positions are identically randomly distributed particles in the unit box. The temporal state of the swarm is updated in time using a numerical scheme called Heun's Method, and a snapshot is captured at every discrete time interval. Here, the left coordinate axis uses a standard deviation of the delays $\sigma_\tau = 0.1$ while the right axis uses

a standard deviation of $\sigma_\tau = 0.3$. The mean delay for each simulation is set to be $\mu_\tau = 2$, and the number of particles for both is $N = 50$. The vectors at each particle give the velocity associated with that particle. The two simulations are run side by side to demonstrate the dynamics involved in converging to the "rotating" final state on the left, and the "ring" final state on the right. The video demonstrates the dynamics over the time interval from $t = 0$ to $t = 45$, and so includes transients.

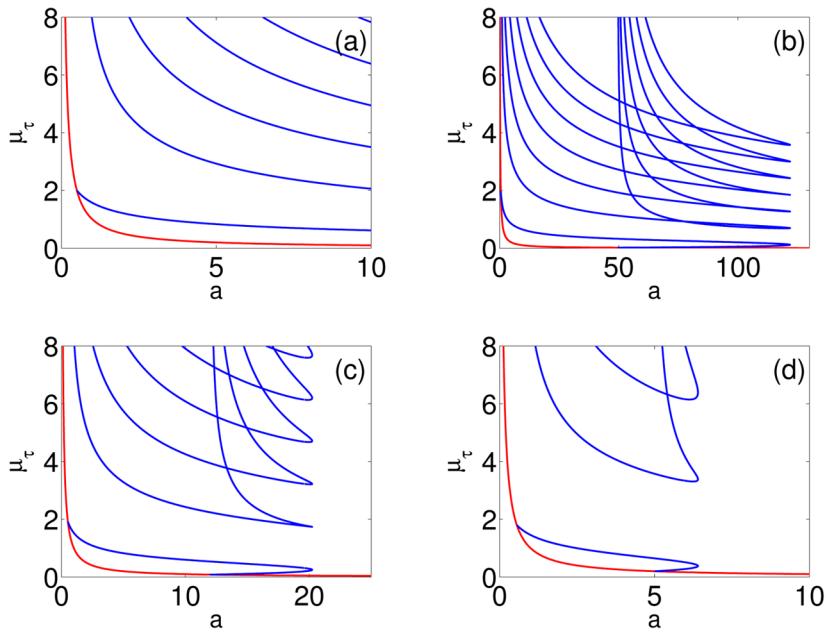

Fig. 1.

Hopf (blue) and pitchfork (red) branches in a and μ_T space. The standard deviations of the time-delay distribution ρ_T for the panels (a) through (d) are 0, 0.2, 0.4 and 0.6, respectively. Note the change of scale in the abscissae.

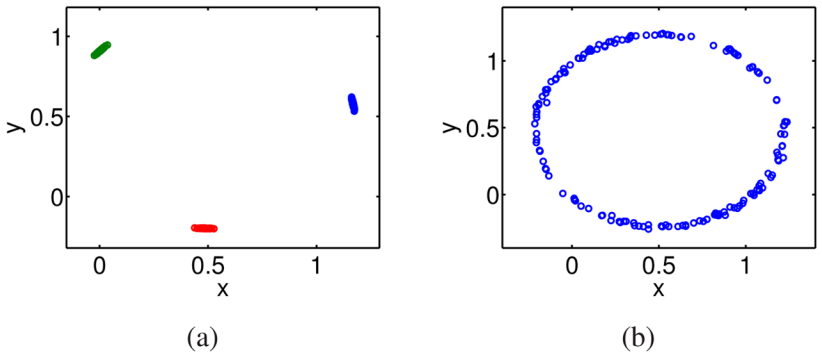

Fig. 2.

Two stable attractors for the swarm dynamics. Here $a = 2$, $\mu_\tau = 2$, and $\sigma_\tau = 0.15$. The number of particles is set to be $N = 150$. The final state shown for both simulations is $t = 300$. Panel (a) depicts the rotating state at three snapshots at times $t = 297.6, 298.8, 300$, in red, green and blue, respectively. Panel (b) depicts the ring state.

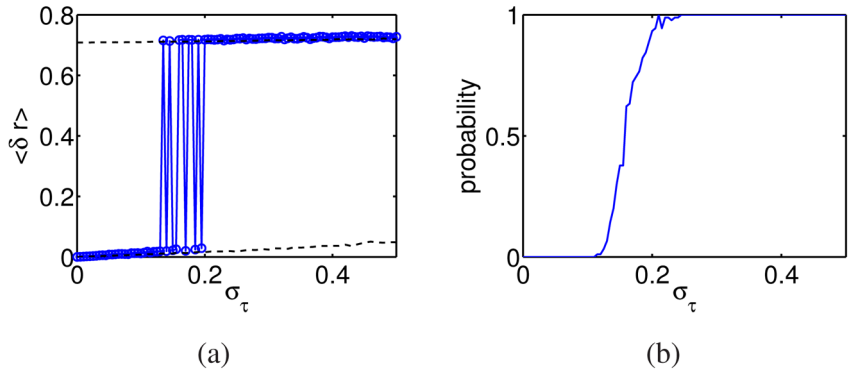

Fig. 3.

As σ_τ is increased, we see a bifurcation from the stable rotating state. Panel (a) captures the transition from the rotating state to the ring state as the standard deviation of the random delay increases. Panel (b) shows the probability of converging to the ring state for a given σ_τ of the delays. These results were compiled using a Monte Carlo simulation with 100 random distributions of delays for 100 uniformly-spaced values of σ_τ and for $N = 50$ particles. See accompanying online movie and Appendix to see the agents converge to each stable pattern.